


ORIGINAL ARTICLE

Commensal microbiota contributes to predicting the response to immune checkpoint inhibitors in non-small-cell lung cancer patients

Chufeng Zhang^{1,2}  | Jixin Wang³ | Zhongwen Sun^{1,4} | Yufeng Cao⁵ | Zhengshuai Mu² | Xuming Ji^{1,6}

¹College of Chinese Traditional Medicine, Shandong University of Traditional Chinese Medicine, Jinan, China

²Shandong Cancer Hospital and Institute, Shandong First Medical University and Shandong Academy of Medical Sciences, Jinan, China

³Zhejiang University-University of Edinburgh Institute, Zhejiang University, Jiaxing, China

⁴Department of Pharmacy, Taishan Hospital of Shandong Province, Taian, China

⁵Qingdao Hiser Hospital Affiliated to Qingdao University, Qingdao, China

⁶Academy of Chinese Medical Science, Zhejiang Chinese Medical University, Hangzhou, China

Correspondence

Xuming Ji, College of Chinese Traditional Medicine, Shandong University of Traditional Chinese Medicine, Jinan, China; Academy of Chinese Medical Science, Zhejiang Chinese Medical University, Hangzhou, China.
Email: jixuming724@163.com

Funding information

Medicine and Health Science Technology Development Project of Shandong Province, Grant/Award Number: 2019WS204; Natural Science Foundation of Shandong Province, Grant/Award Number: ZR2020QH209; National Natural Science Foundation of China, Grant/Award Number: 81774198 and 81573871

Abstract

Immunotherapy against cancer, through immune checkpoint inhibitors targeting the programmed cell death-1/programmed cell death-ligand 1 axis, is particularly successful in tumors by relieving the immune escape. However, interindividual responses to immunotherapy are often heterogeneous. Therefore, it is essential to screen out predictive tumor biomarkers. In this study, we analyzed the commensal microbiota in stool samples and paired sputum samples from 75 metastatic non-small-cell lung cancer (NSCLC) patients at baseline and during treatment with immune checkpoint inhibitors. Results showed distinct microbes' signatures between the gut microbiota and paired respiratory microbiota. The alpha diversity between the gut and respiratory microbiota was uncorrelated, and only the gut microbiota alpha diversity was associated with anti-programmed cell death-1 response. Higher gut microbiota alpha diversity indicated better response and more prolonged progression-free survival. Comparison of bacterial communities between responders and nonresponders showed some favorable/unfavorable microbes enriched in responders/nonresponders, indicating that commensal microbiota had potential predictive value for the response to immune checkpoint inhibitors. Generally, some rare low abundance gut microbes and high abundance respiratory microbes lead to discrepancies in microbial composition between responders and nonresponders. A significant positive correlation was observed between the abundance of *Streptococcus* and CD8⁺ T cells. These results highlighted the intimate relationship between commensal microbiota and the response to immunotherapy in NSCLC patients. Gut microbiota and respiratory microbiota are promising biomarkers to screen suitable candidates who are likely to benefit from immune checkpoint inhibitor-based immunotherapy.

Abbreviations: BMI, body mass index; ICI, immune checkpoint inhibitor; LefSe, linear discriminant analysis effect size; LRT, lower respiratory tract; MW, Mann-Whitney; NCCN, National Comprehensive Cancer Network; NR, nonresponder; NSCLC, non-small-cell lung cancer; PCoA, principal coordinate analysis; PD, progressive disease; PD-1, programmed cell death-1; PD-L1, programmed cell death-ligand 1; PFS, progression-free survival; PR, partial response; PS, performance status; R, responder; ROC, receiver operating characteristic; SD, stable disease; TIL, tumor infiltrating lymphocyte; TMB, tumor mutation burden; TPS, tumor proportion score; URT, upper respiratory tract.

This is an open access article under the terms of the Creative Commons Attribution-NonCommercial-NoDerivs License, which permits use and distribution in any medium, provided the original work is properly cited, the use is non-commercial and no modifications or adaptations are made.

© 2021 The Authors. *Cancer Science* published by John Wiley & Sons Australia, Ltd on behalf of Japanese Cancer Association.

KEYWORDS

immune checkpoint inhibitor, microbiota, non-small-cell lung cancer, programmed cell death-1, progression-free survival

1 | INTRODUCTION

The development and progression of cancer are associated with the failure of immune surveillance. Immune checkpoint inhibitor-based immunotherapy is capable of relieving the immune escape and has since been approved by NCCN guidelines.¹⁻⁵ T lymphocyte-mediated responses can potentially be unleashed by ICIs via inhibiting the interaction between T cell inhibitory receptors and their homologous ligands on tumor cells.⁶ However, interindividual responses to ICIs are often heterogeneous.^{7,8} Primary resistance has been attributed to low PD-L1 tumor proportion score,⁹ low TMB,¹⁰ poor intrinsic antigenicity of tumor cells,¹¹ local immunosuppression by extracellular metabolites,¹² defective antigen presentation during the priming phase,¹³ and functional exhaustion of tumor-infiltrating lymphocytes.^{14,15} In recent years, increasing evidence has revealed that the commensal microbiota is an important biological factor contributing to interindividual heterogeneity of response to ICIs. Clinical/preclinical studies have indicated that the composition of the gut microbiota can exert a significant influence on antitumor immunity and immunotherapy efficacy.¹⁶⁻¹⁹

However, current studies seem to lack consensus on what are the favorable or unfavorable microbes to ICIs. Sivan et al found that commensal gut *Bifidobacterium* promoted antitumor immunity and facilitated anti-PD-L1 efficacy for melanoma cancer.¹⁹ Matson et al found high abundant gut *Bifidobacterium longum*, *Collinsella aerofaciens*, and *Enterococcus faecium* were associated with better anti-PD-1 efficacy in metastatic melanoma patients.¹⁸ Jin et al found that clinical responses to ICIs were associated with the relative abundance of *Alistipes putredinis*, *Bifidobacterium longum*, *Prevotella copri*, and unclassified *Ruminococcus* in NSCLC.²⁰ Therefore, these mixed results from limited eligible studies need more in-depth research on the relationship between gut microbiota and the response to ICIs in cancer patients. Additionally, nearly all research has predominantly focused on gut microbiota and its influence on host immunity. The relationship between respiratory microbiota and the response to ICIs in NSCLC has not been widely explored, even though the respiratory microbiota has been found to provoke inflammation associated with lung cancer.²¹ The respiratory tract can be divided into the URT and LRT. The URT includes the portion of the larynx above the vocal cords, oropharynx, nasopharynx, paranasal sinuses, nasal passages, and anterior nares. The LRT includes the portion of the larynx below the vocal cords, the trachea, smaller airways, and alveoli. Respiratory microbiota can be defined as the microbe community present in the respiratory tract. This study was designed to evaluate the relationship between the commensal microbiota (gut microbiota and paired respiratory microbiota) and the clinical efficacy of ICIs in advanced NSCLC patients and also assess their potential value as new biomarkers in predicting the response to immunotherapy.

2 | MATERIALS AND METHODS

2.1 | Patient cohort

Metastatic NSCLC patients suffering from a failure of platinum-based chemotherapy and were to receive anti-PD-1 monotherapy were enrolled in this study between May 2019 and January 2021 at Shandong Cancer Hospital (Figure 1). All the study participants had measurable lesions according to RECIST 1.1.²² Patients with active or not pretreated brain metastases were excluded from this study. Baseline patients who had not recovered from physical symptoms of acute diarrhea were also excluded from this analysis. Medical images were reviewed independently by two radiologists for appraisal of clinical response according to the updated RECIST 1.1.²³ Patients were classified as R if they achieved complete response, PR, or SD lasting at least 6 months, and patients were classified as NR if they suffered PD (confirmed by a subsequent assessment no less than 4 weeks from the first evaluation) or SD lasting less than 6 months. This classification considers those patients who would benefit from immunotherapy over the long term despite not achieving a RECIST response. It is more accurate and rigorous in estimating disease progression for a subset of patients who suffer pseudo-progression, which is defined as a more than 30% decrease in the total size of tumor target lesions from the baseline after PD. This classification method is widely used in published studies.^{24,25} Patients' demographic, clinical, pathological, and molecular data were extracted from the medical records, including tumor characteristics, the number of metastatic sites, PD-L1 expression when available, previous treatment, driver mutation, and ECOG PS scores. All patients had been given full access to information and consented to participate in this observational study. The procedures involved in the collection and analysis of stool samples, sputum samples, and biopsy samples were approved by the ethics committee of Shandong Cancer Hospital. All the procedures were carried out following the principals of the Declaration of Helsinki.

2.2 | Stool samples and paired sputum samples collection

At least 1 g of stool and paired sputum samples were collected in sterile specimen containers before anti-PD-1 treatment. Considering that sputum samples were inevitably contaminated by the oral cavity during the sampling process, we took additional samples in the oral cavity as controls in some patients. For oral cavity sampling, we used a swab to quickly wipe the oral cavity mucosa on the medial side of the cheek, and put the swab into a sterile tube. The samples were transported to the laboratory within 2 hours after collection. Eligible patients were provided with a Fecal Sample Collection Kit (CY-98000PFB) and Sputum Sample Collection Kit (CY-98000A) (Huachenyang) for collection of stool and

sputum samples at home. These kits maintain microbial DNA stability at 15–30°C for up to 12 months. All samples were frozen at –80°C before DNA extraction and analysis. Usually, stool samples should be collected in the mid-posterior section of the feces; sputum samples should be collected in the early morning after a deeply forceful cough. All sampling time points have avoided special cases, such as emerging diarrhea. For details such as DNA extraction, PCR amplification, Illumina MiSeq sequencing, and bioinformatics analysis, see Materials in Supporting Information.

2.3 | Statistical analyses

Statistical analyses were undertaken using SPSS 22.0 (IBM). Patients' baseline characteristics are described according to the objective response of anti-PD-1 treatment and data compared using Pearson's χ^2 test or continuous correction χ^2 test. In general, the nonparametric Kruskal-Wallis test or MW test was used to compare abundance and alpha diversity between groups. Spearman's rank correlation test was used to detect the correlation of pairwise data. Kaplan-Meier survival analysis was used to assess median PFS in each group, and any differences in PFS were evaluated with a stratified log-rank (Mantel-Cox) test. The Friedman test was used to compare the Shannon index at different time points. Beta diversity analysis of the differences in microbiota community between R and NR was carried out using analysis of similarities.

3 | RESULTS

3.1 | Baseline patient characteristics

An initial cohort of 91 patients with advanced NSCLC was included in this study. Patients who received PD-1 inhibitors combined with

targeted therapy ($n = 8$) or radiotherapy ($n = 8$) in the treatment course were excluded from this analysis. Finally, 75 patients were eligible for analysis (Figure 1). The 75 patients were classified into R ($n = 25$, including 21 PR patients and 4 SD patients) and NR ($n = 50$, including 20 SD patients and 30 PD patients). A total of 75 stool samples and 57 sputum samples were collected at baseline (Figure 1). Baseline characteristics of the 75 patients are presented in Table 1. Variables that are considered to influence the anti-PD-1 effect, such as smoking,¹⁷ steroid use,²⁶ antibiotic use,²⁷ radiotherapy history,²⁸ and *EGFR* mutations status²⁹ were relatively balanced between R and NR. Increasing evidence has indicated that PD-L1 TPS and TMB are factors influencing anti-PD-1 treatment; thus, we recorded TMB and detected PD-L1 status in eligible patients. Of the 75 patients, 67 patients' biopsies qualified for high-quality PD-L1 analysis by immunohistochemistry. Forty-two patients showed positive expression (PD-L1 TPS ≥ 1), of which 16 patients showed high positive expression (PD-L1 TPS $\geq 50\%$), and 26 patients showed low positive expression ($1\% \leq$ PD-L1 TPS $< 50\%$). There was no statistical difference between groups. Thirteen patients underwent TMB detection by next generation sequencing in tumor tissue specimens, and the results showed that TMB ranged from 15.8/Mb to 53.4/Mb. No differences in TMB were observed between R and NR (Figure S1).

3.2 | Differences in commensal microbiota landscape and abundance between gut microbiota and respiratory microbiota

Microbes are well-annotated at kingdom, phylum, class, order, family, and genus level (Figure S2). We first compared the microbiota diversity by 16S sequencing based on paired samples (stool samples and paired sputum samples) from 15 patients, noting that both gut and

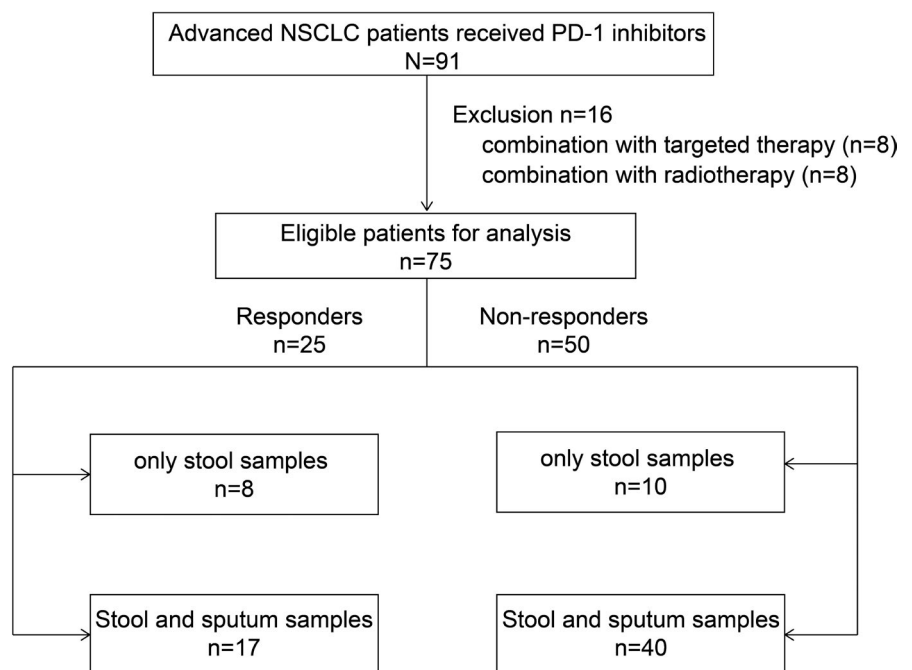


FIGURE 1 Schema of patient enrollment and sample collection. NSCLC, non-small-cell lung cancer; PD-1, programmed cell death-1

TABLE 1 Baseline characteristics of 75 patients with advanced non-small-cell lung cancer classified as treatment responders (R) or nonresponders (NR)

| Characteristic | R (n = 25) | NR (n = 50) | P value |
|--------------------------------|------------|-------------|---------|
| Age, years | | | |
| ≤60 | 15 (60.0) | 27 (54.0) | .62 |
| >60 | 10 (40.0) | 23 (46.0) | |
| Gender | | | |
| Male | 16 (64.0) | 29 (58.0) | .62 |
| Female | 9 (36.0) | 21 (42.0) | |
| Smoking history | | | |
| Yes | 11 (44.0) | 21 (42.0) | .87 |
| Never | 14 (56.0) | 29 (58.0) | |
| Alcohol drinking history | | | |
| Yes | 16 (64.0) | 28 (56.0) | .51 |
| No | 9 (36.0) | 22 (44.0) | |
| BMI | | | |
| >24 | 6 (24.0) | 15 (30.0) | .59 |
| ≤24 | 19 (76.0) | 35 (70.0) | |
| Histopathology | | | |
| Squamous carcinoma | 13 (52.0) | 27 (54.0) | .87 |
| Adenomatous carcinoma | 12 (48.0) | 23 (46.0) | |
| ECOG PS scores | | | |
| ≤1 | 18 (72.0) | 34 (62.0) | .72 |
| >1 | 7 (28.0) | 16 (38.0) | |
| History of steroid hormone use | | | |
| Yes | 8 (32.0) | 20 (40.0) | .50 |
| No | 17 (68.0) | 30 (60.0) | |
| History of antibiotic use | | | |
| Yes | 10 (40.0) | 17 (34.0) | .61 |
| No | 15 (60.0) | 33 (66.0) | |
| Number of metastatic sites | | | |
| ≤3 | 15 (60.0) | 21 (42.0) | .14 |
| >3 | 10 (40.0) | 29 (58.0) | |
| EGFR mutation status | | | |
| WT | 22 (88.0) | 45 (90.0) | 1.0 |
| Mutant type | 3 (12.0) | 5 (10.0) | |
| History of radiotherapy | | | |
| Yes | 15 (60.0) | 21 (42.0) | .14 |
| No | 10 (40.0) | 29 (58.0) | |
| Type of PD-1 inhibitor | | | |
| Nivolumab | 11 (44.0) | 25 (50.0) | .62 |
| Pembrolumab | 14 (56.0) | 25 (50.0) | |
| PD-L1 status | | | |

(Continues)

TABLE 1 (Continued)

| Characteristic | R (n = 25) | NR (n = 50) | P value |
|---------------------------------------|------------|-------------|---------|
| PD-L1 TPS ≥ 50% (high expression) | 7 (31.8) | 9 (20.0) | .35 |
| 1% ≤ PD-L1 TPS < 50% (low expression) | 6 (27.3) | 20 (44.4) | |
| PD-L1 TPS < 1% (negative expression) | 9 (40.9) | 16 (35.6) | |

Note: Data are shown as n (%). Patient classification: NR, progressive disease, or stable disease for <6 months; R, complete response, partial response, or stable disease for ≥6 months.

Abbreviations: BMI, body mass index; PD-1, programmed cell death-1; PD-L1, programmed cell death-ligand 1; PS, performance status; TPS, tumor proportion score.

^aHistory of drug use limited to within 1 mo.

respiratory microbiota were relatively diverse (Shannon index > 5) (Figure 2A). No significant difference in Shannon alpha diversity was observed between the two groups. However, the landscape of the 20 genus microbes ranking the top 20 abundance at baseline varied markedly (Figure 2B). Only a small fraction of microbial species were shared between the gut and respiratory microbiota (Figure 2C). ANCOM showed that the abundance of most of the common species was significantly different between the two communities (Figure 2D). Beta diversity analysis and clustering based on microbe abundance confirmed a distinct microbiota community composition between the gut and respiratory microbiota (Figure 2D,E).

3.3 | Gut microbiota diversity is associated with anti-PD-1 response

Previous discoveries have indicated that the gut microbiota has a significant influence on the efficacy of ICIs in melanoma. Therefore, we sought to ascertain whether this influence existed in NSCLC; in particular, to identify the relationship between respiratory microbiota and anti-PD-1 response. We analyzed the diversity of gut and respiratory microbiota at baseline. Results showed that the alpha diversity (measured by the Chao1 index and Shannon index) of the gut microbiota was significantly higher in R than NR. However, no significant difference was observed when referred to the Simpson alpha diversity index (Figure 3A). No statistical difference of alpha diversity was observed between R and NR in respiratory microbiota ($P > .05$, MW test). Further research on the 15 stool samples and paired sputum samples showed that alpha diversity between the two microbial communities was uncorrelated ($P > .05$, Spearman's test). Subgroup analysis revealed that the differences in the gut microbiota between R and NR were mainly caused by PR and PD patients when measured by Chao1 index and Shannon index (Figure 3B). The patients were stratified into two cohorts based on the cut-off value (Shannon index = 5.75) obtained from the ROC curve (Figure S3). Results

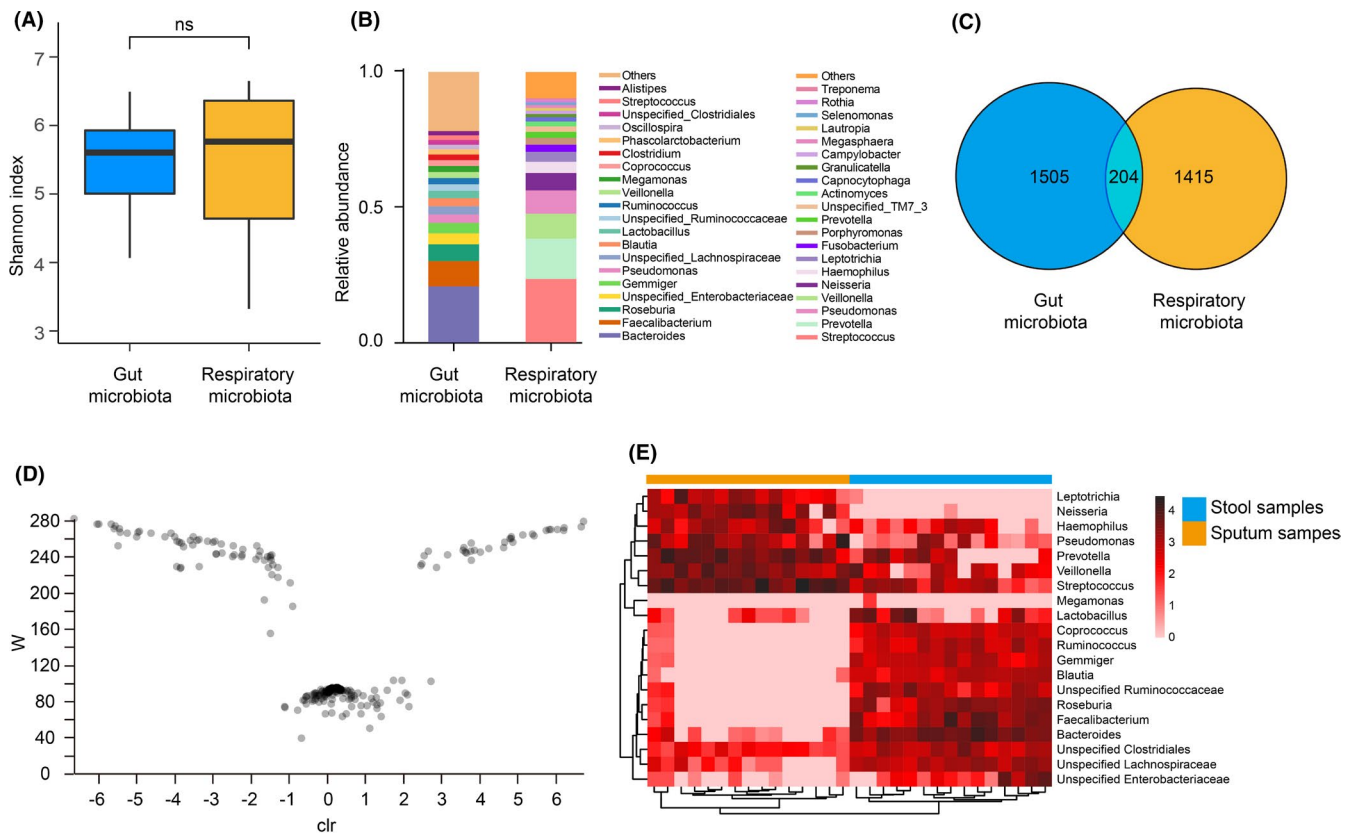


FIGURE 2 Difference in composition between gut and respiratory microbiota in patients with non-small-cell lung cancer. All microbial data are obtained from stool samples and paired sputum samples in 15 patients. A, Boxplot of Shannon index (alpha diversity). Shannon diversity index for gut microbiota and respiratory microbiota is 5.61 and 5.76, respectively. ns, $P > .05$ by Mann-Whitney test. B, Microbial landscape and the relative abundance of gut microbes and respiratory microbes at the genus level. C, Venn diagrams showing common species. Two circles represent species counts of gut species ($n = 1505$) and respiratory species ($n = 1415$). Overlap area represents common species ($n = 204$). D, Analysis of composition of microbiomes (ANCOM) by volcano plot to compare the differences in the abundance of common species. Each plot in the diagram represents a compared species. E, Heatmap of unsupervised hierarchical clustering of microbes at the genus level. Gradation of color represents the level of microbes' relative abundance (\log_{10}). W value from ANCOM is a statistic that measures the significance of differences between groups, and the clr value from ANCOM represents the degree of abundance difference between groups

showed that patients harboring a higher alpha diversity had a higher response rate (60.0% vs 22.5%, $P < .01$) and significantly prolonged median PFS (4.6 months vs 3.3 months, $P = .02$) (Figure 3C,D). It is also important to note that the Simpson index, compared with other alpha diversity indices, showed minimal differences between the two groups (Figure 3A,B). According to the formula used to calculate the indices, rare low abundance microbes had minimal weights on the Simpson index relative to Chao1 and Shannon indices.^{30,31} Thus, we assumed that the alpha diversity difference between R and NR might be caused by the rare low abundance microbes. This assumption was consistent with a previous finding that rare low abundance microbes were associated with anti-PD-1 response and CD8⁺ T cell immunity in melanoma cancer.^{16,32}

We estimated the beta diversity of the gut microbiota in R and NR. Through visual comparison by PCoA based on unweighted UniFrac and supervised partial least squares-discriminant analysis, we found that there was a statistical difference between R and NR, even though the unweighted PCoA showed a less obvious clustering effect (Figure S4A). However, weighted UniFrac PCoA showed

no difference in beta diversity between R and NR. Different results from unweighted and weighted PCoA analyses indicated that low abundance microbe composition might differ between the two groups. The relationship between respiratory microbiota and the different anti-PD-1 response was estimated. Unlike the gut microbiota, the weighted UniFrac PCoA showed a statistical difference in beta diversity between R and NR (Figure S4B), indicating that some respiratory microbes with high abundance might greatly contribute to the difference in beta diversity between R and NR.

3.4 | Featured microbes in R and NR

To further investigate the featured microbes in R and NR, we used LEfSe. Results indicated differentially abundant gut microbes in R versus NR to anti-PD-1 response, with *Desulfovibrio*, Actinomycetales, *Bifidobacterium*, Odoribacteraceae, *Anaerostipes*, Rikenellaceae, *Faecalibacterium*, and *Alistipes* enriched in R, whereas Fusobacterales, Fusobacteriia, *Fusobacterium*, Fusobacteria, and

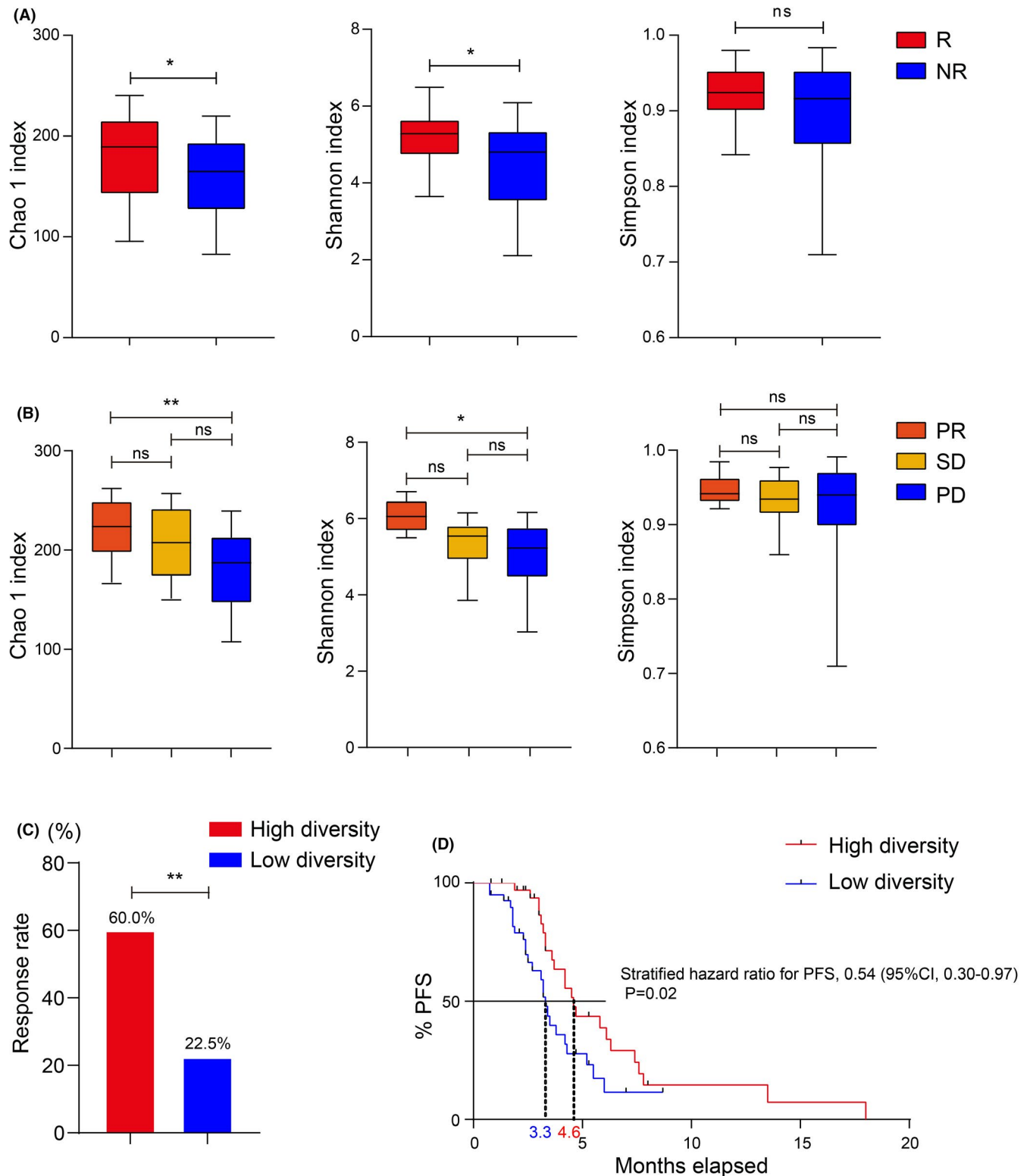


FIGURE 3 Alpha diversity of the gut microbiota in patients with non-small-cell lung cancer is associated with anti-PD-1 response and progression-free survival (PFS). A, Diversity index between treatment responders (R) and nonresponders (NR). Three graphs from left to right show the Chao1, Shannon, and Simpson index, respectively. * $P < .05$, ** $P < .01$ by Mann-Whitney (MW) test. B, Subgroup analysis of diversity in the gut microbiota among patients with partial response (PR), stable disease (SD), and progressive disease (PD). * $P < .05$, ** $P < .01$ by MW test. C, Response rate in the high diversity group ($n = 35$) vs low diversity group ($n = 40$) with a cut-off value of the Shannon index (5.75) from the receiver operating characteristic curve. ** $P < .01$ by Pearson's χ^2 test. D, Kaplan-Meier survival analysis of PFS in the high and low diversity groups. The median PFS of the high diversity and low diversity group was 4.6 and 3.3 mo, respectively. $P = .02$ by log-rank Mantel-Cox test; hazard ratio, 0.54 (95% confidence interval, 0.30-0.97). ns, $P > .05$

Fusobacteriaceae were enriched in NR (Figure 4A,B). We analyzed the relative abundance of these microbes in the corresponding taxon level and found that nearly all were in low abundance (Table S1). However, respiratory microbiota showed the opposite characteristics, where some featured microbes in R and NR were abundant, such as Firmicutes and Proteobacteria (Figure 4C,D and Table S1).

These results further supported the suggestion that some gut microbes with low abundance and respiratory microbes with high abundance might lead to the discrepancy in bacterial composition between R and NR.

To assess the value of the featured microbes as biomarkers in predicting the anti-PD-1 response, we evaluated all featured

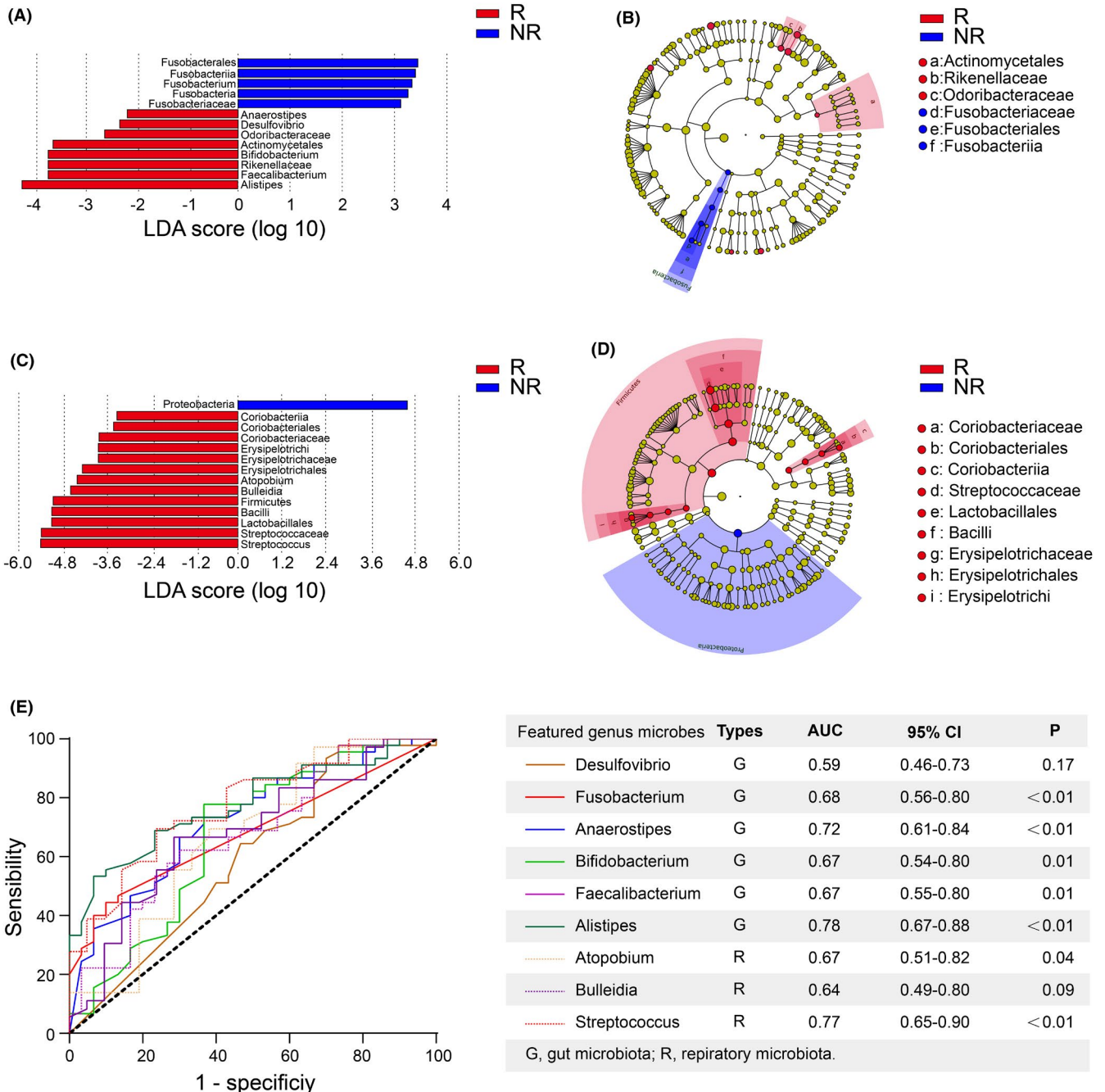


FIGURE 4 Featured microbes in patients with non-small-cell lung cancer classified as treatment responders (R) or nonresponders (NR). A, C, Linear discriminant analysis (LDA) histogram from linear discriminant analysis effect size (LefSe). The length of the histogram represents LDA scores computed for differentially abundant microbes in (A) gut microbiota and (C) respiratory microbiota of R (red) and NR (blue). $P = .05$ by Kruskal-Wallis test; LDA score >2 . B, D, Taxonomic cladogram from LefSe showing differences in (B) gut microbiota and (D) respiratory microbiota. Dot size is proportional to the abundance of the microbe. Red dots indicate a significant difference in abundance between the two groups ($P < .05$ by Kruskal-Wallis test). Yellow dots indicate no significant difference in abundance between the two groups. E, Multi-index receiver operating characteristic (ROC) curves to assess the value of microbes of featured genera as biomarkers in predicting anti-PD-1 response. AUC, area under the ROC curve; CI, confidence interval

genera of gut microbes (*Fusobacterium*, *Anaerostipes*, *Desulfovibrio*, *Bifidobacterium*, *Faecalibacterium*, and *Alistipes*) and respiratory microbes (*Atopobium*, *Bulleidia*, and *Streptococcus*) by ROC curves. Results showed a good predictive value of the abundance of these featured microbes, except *Desulfovibrio* and *Bulleidia* (Figure 4E). According to cut-off values from ROC curves, the patients were divided into two groups, and we compared response rates and PFS between groups. We found a significant difference in response rate between groups for most microbes (Table S2). However, only *Fusobacterium* (gut microbiota) and *Streptococcus* (respiratory microbiota) showed differences in median PFS between the high and low abundance groups.

3.5 | Diversity and abundance of gut and respiratory microbes maintain stability during anti-PD-1 treatment

As described above, the baseline gut and respiratory microbiota profiles were associated with anti-PD-1 response in NSCLC. We

attempted to investigate further whether the profiles were steady throughout the entire treatment. Therefore, a longitudinal sampling strategy was carried out to dynamically evaluate the gut and respiratory microbe landscape and abundance in 15 eligible patients. Sampling time points were at baseline before treatment (T0), from the first to fourth treatment cycle (T1-T4), and when the disease progressed (Tp). Alpha and beta diversity at different time points were analyzed. Results showed that there was no significant difference in alpha diversity among T0, T1, T2, T3, T4, and Tp time points for both gut and paired respiratory microbiota ($P > .05$) (Figure 5A). Additionally, there was no significant difference in beta diversity and no pronounced clustering effect between T0 and Tp time points (Figure 5B,C), indicating that no significant alterations occurred in the phylogenetic tree throughout the anti-PD-1 treatment. Finally, 20 microbes were selected, all ranked in the top 20 most abundant at baseline, and their variation in abundance in each patient was observed at the Tp time point. Intuitively, the relative abundance of these microbes changed little (Figure 5D,E). These results indicated that gut and respiratory microbiota profiles maintain relative stability during the entire anti-PD-1 treatment.

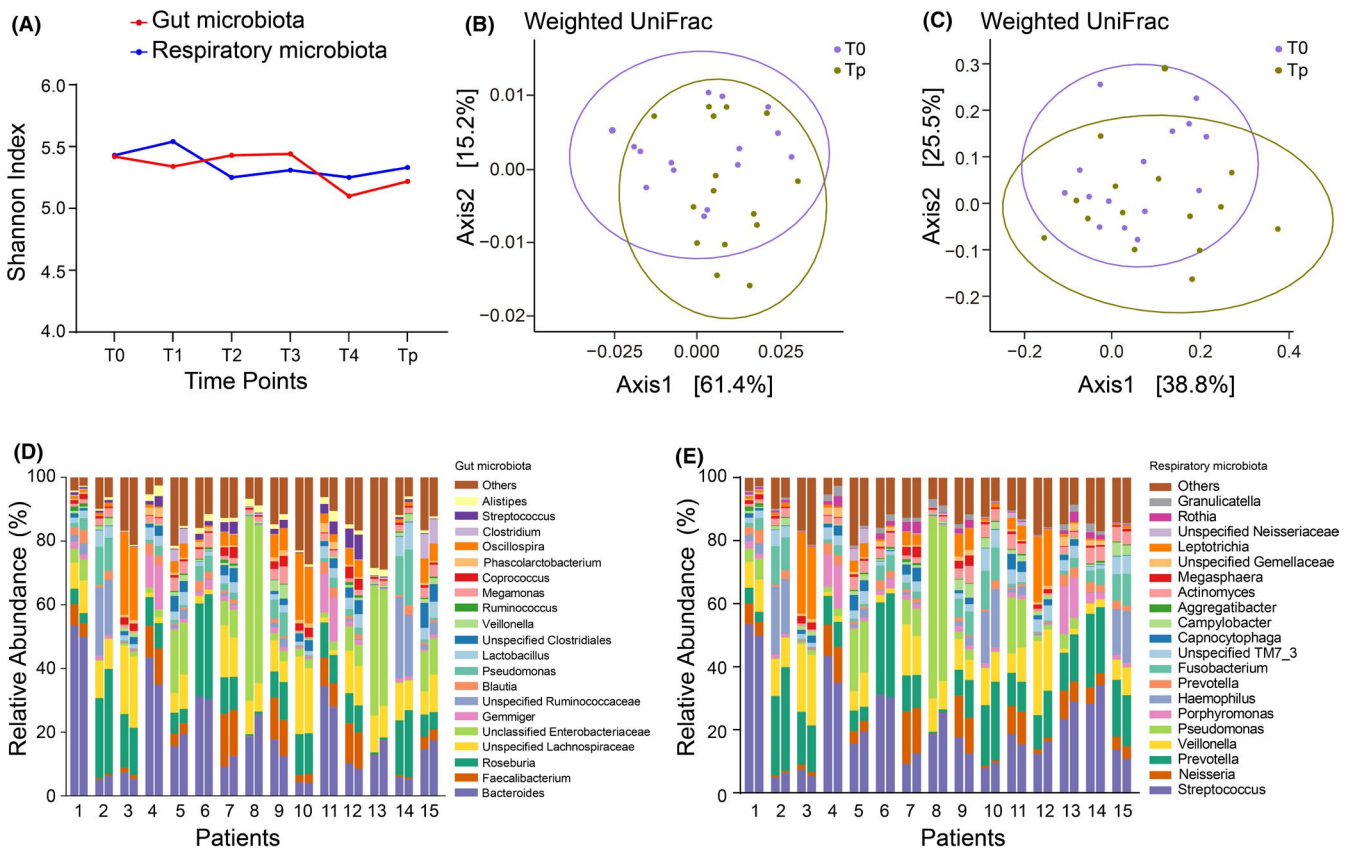


FIGURE 5 Alpha diversity and abundance of the gut and respiratory microbiota maintain stability during anti-PD-1 treatment in patients with non-small-cell lung cancer. A, Alpha diversity (measured by Shannon index) of gut and respiratory microbiota at different time points (from baseline [T0] to disease progression [Tp]). $P > .05$ by Friedman test. B, C, Beta diversity (measured by principal coordinate analysis) comparison at T0 and Tp time points for (B) gut microbiota and (C) respiratory microbiota. $P > .05$ by analysis of similarities. D, E, Abundance variation of 20 microbes at T0 and Tp time points in 15 patients. Each microbe was ranked in the top 20 in terms of average abundance at baseline in the gut and respiratory microbiota. For every patient (1–15), the bar plot on the left represents the T0 time point, and on the right represents the Tp time point

3.6 | Relationship between commensal microbiota, anti-PD-1 response, and clinical variables

As baseline gut and respiratory microbiota profiles were associated with an anti-PD-1 response, we sought to ascertain the possible clinical variables that influenced the distribution of microbes between R and NR. In this study, several clinical variables we put into consideration, such as ECOG PS scores, age, smoking index, average alcohol consumption, and BMI. Results of redundancy analysis showed that PS scores, alcohol consumption, and BMI were important clinical variables that influenced the distribution of gut microbes between R and NR (Figure 6A). Interestingly, we found that nearly all gut microbes featured in R or NR at the genus level were influenced by PS scores (Figure 6B). Better PS indicated a higher abundance of favorable microbes (eg, *Alistipes*, *Anaerostipes*, and *Desulfovibrio*) that featured in R and a lower abundance of unfavorable microbes (such as *Fusobacterium*) that featured in NR. Smoking and alcohol consumption were associated with a lower abundance of favorable microbes, such as *Bifidobacterium* and *Anaerostipes*. Alcohol consumption was also associated with a higher abundance of unfavorable *Fusobacterium*, and elderly patients were associated with a lower abundance of favorable *Bifidobacterium*. Better physical condition, young age, less smoking, and less alcohol consumption seemed to improve the abundance of favorable microbes featured in R or reduce the abundance of unfavorable microbes featured in NR.

However, no clinical variable was observed for respiratory microbiota to affect the distribution of microbes between R and NR (Figure 6C). Those respiratory microbes at the genus level featured in R and NR were also unaffected by the above clinical variables (Figure 6D).

3.7 | Relationship between respiratory microbes and TILs

As the gut microbiota has been confirmed to control anti-PD-1 response by regulating the tumor microenvironment,^{16,19,33} we investigated tumor-associated TILs by immunohistochemistry. Consistent with previous reports, we observed a high density of CD8⁺ T cells in R versus NR (Figure 7A). We then undertook pairwise comparisons using Spearman rank correlations between CD8⁺ T cells, CD4⁺ T cells, IFN- γ ⁺CD4⁺ T cells (Th1), IL-4⁺CD4⁺ T cells (Th2), FoxP3⁺CD4⁺ T cells (Treg cells), and the abundance of respiratory microbes featured in R or NR. A statistically significant positive correlation was observed between the abundance of *Streptococcus* and CD8⁺ T cells density (Figure 7B,C). No associations were seen between other genus respiratory microbes and the density of CD8⁺ T cells. Representative CD8⁺ immunohistochemistry images in high and low abundance of *Streptococcus* groups are presented in Figure 7D.

4 | DISCUSSION

This study found that the alpha diversity between the gut and respiratory microbiota was uncorrelated in patients with NSCLC, and only the gut microbiota alpha diversity was associated with anti-PD-1 response and PFS. The beta diversity in both the gut and respiratory microbiota was statistically different between R and NR. The diversity of microbiota is affected by biotic and abiotic drivers and, in turn, affects ecosystem functioning. Nevertheless, patterns of diversity in host-associated microbiota are poorly studied. Diet, age, lifestyle, drugs, and body size are generally considered to affect diversity in the gut, but gut physiology is deemed the most important driver.^{34,35} Respiratory microbiota was also influenced by host and environmental factors, such as genetics, smoking, vaccination, infection, and antibiotics.³⁶ In general, the diversity difference among individuals is the result of the interaction of many factors. Compared with other tumor biomarkers, such as PD-L1 and TMB, the commensal microbiota is plastic. Evidence showed that anti-PD-1 response could be improved by increasing the alpha diversity or improving the abundance of specific microbes.^{16,17,19} Some rare low abundance gut microbes and high abundance respiratory microbes might contribute to the discrepancy in diversity between R and NR. Our findings were not consistent with results reported in previous studies regarding what were the favorable or unfavorable gut microbes. In this study, *Alistipes*, *Anaerostipes*, *Desulfovibrio*, *Faecalibacterium*, and *Bifidobacterium* were favorable, whereas *Fusobacterium* was an unfavorable microbe for anti-PD-1 treatment. A high abundance of *Alistipes*, *Faecalibacterium*, and *Bifidobacterium* has also been found to be associated with better anti-PD-1 response in other studies.^{16,19,20} Currently, the mechanisms that favorable gut microbes use to modulate antitumor immunity are not clear. However, some studies have shown that favorable gut microbes affect antigen processing and presentation within the tumor microenvironment.^{16,19,20} Favorable gut microbes enhance systemic and antitumor immune responses mediated by increased antigen presentation and improved effector T cell function in the periphery and tumor microenvironment. However, there is a dearth of information about what are unfavorable gut microbes for ICIs. Our results showed that *Fusobacterium* was an important unfavorable gut microbe (Figure 5A). *Fusobacterium* was found highly enriched in primary and paired metastasis in colorectal cancer patients and involved in tumor metastasis.^{37,38} *Fusobacterium* increases tumor multiplicity and selectively recruits tumor-infiltrating myeloid cells, promoting tumor progression.³⁹ *Fusobacterium* also promotes cancer resistance to chemotherapy by modulating autophagy.⁴⁰ Thus, *Fusobacterium* seems to be an unfavorable factor for tumor prevention and treatment. However, further investigations are required to reveal the relationship between *Fusobacterium* and anti-PD-1 response. For respiratory microbiota, few studies have addressed the relationship between respiratory microbiota and anti-PD-1 response. However, we found that some microbes were enriched in

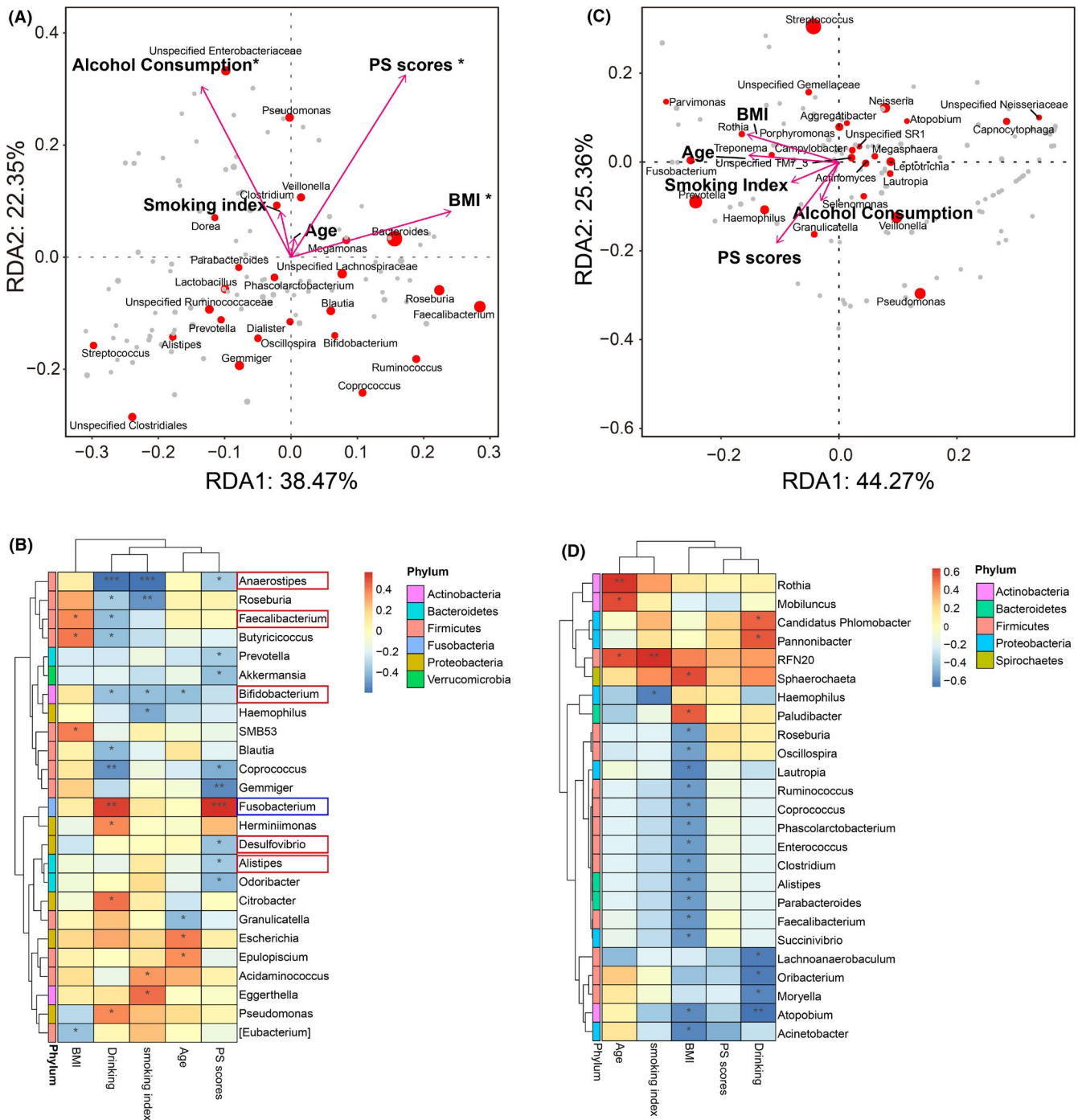


FIGURE 6 Redundancy analysis (RDA) and correlation heatmap showing clinical variables influencing the distribution of microbes in patients with non-small-cell lung cancer classified as treatment responders (R) or nonresponders (NR). A, C, RDA of clinical variables in (A) gut microbiota and (C) respiratory microbiota. Each dot represents a microbe at the genus level. Dot size is proportional to the abundance of the microbe. *Clinical variables with a statistical influence on the distribution of microbes between R and NR; $P < .05$ by permutation test. Gray dots without labeling represent low abundance microbes. B, D, Correlation heatmap between microbe abundance (B, gut microbiota; D, respiratory microbiota) and clinical variables. Spearman's correlation coefficients (r value) are shown with continuous gradient colors. $*0.01 \leq P < .05$, $**0.001 \leq P < .01$, $***P < .001$. Red boxes indicate favorable gut microbes featured in R; blue boxes indicate unfavorable gut microbes featured in NR. BMI, body mass index; PS, performance status

R or NR, even though there was no difference in alpha diversity between R and NR (Figure 5C,D). Featured microbes might potentially influence the anti-PD-1 response through the tumor immune microenvironment, as we observed a positive correlation between

the abundance of *Streptococcus* and CD8⁺ T cells. Thus, this is an attractive direction that warrants further research. However, there is a certain flaw in our study, that is, our sputum samples were inevitably contaminated with saliva. Although sampling

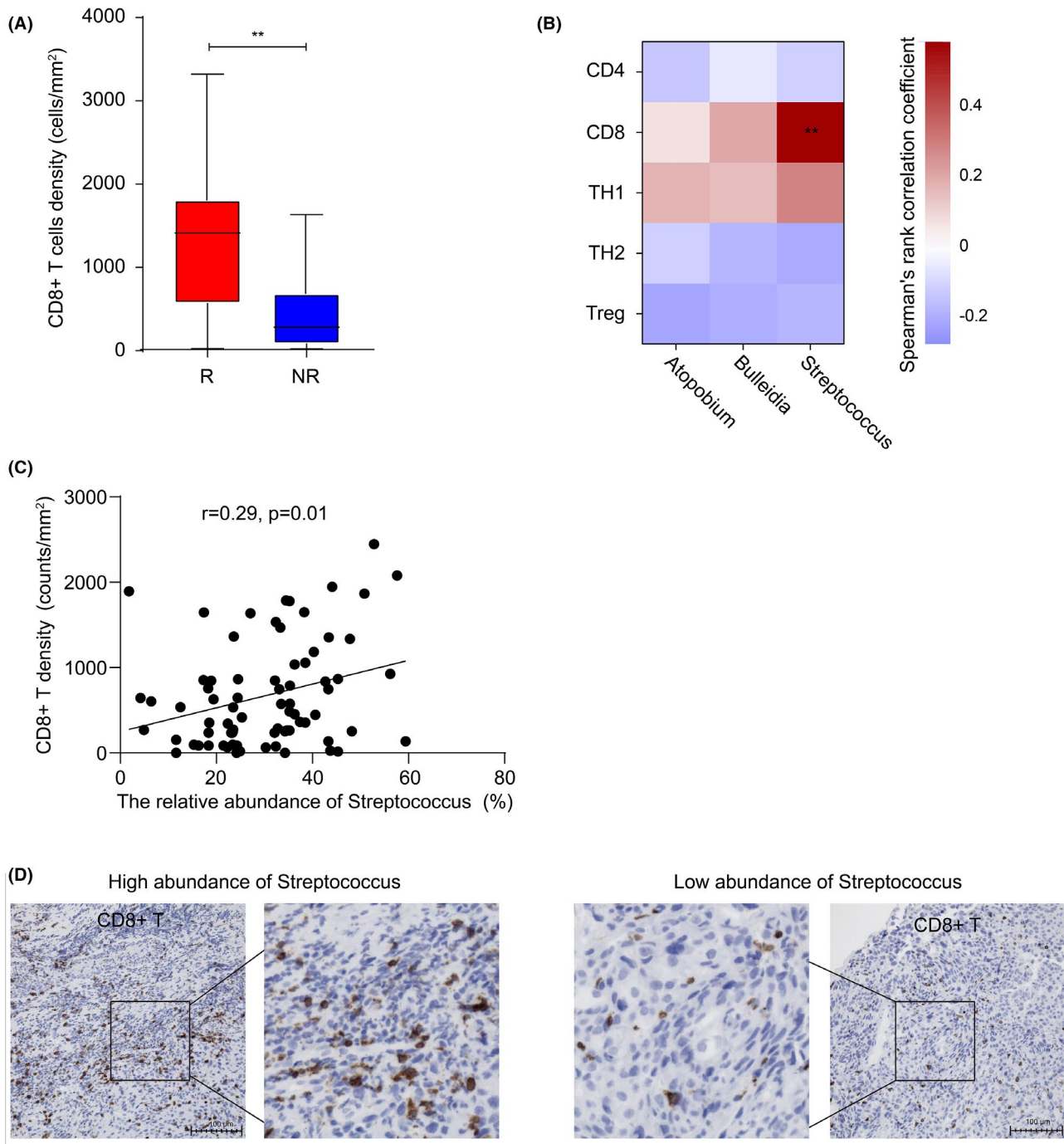


FIGURE 7 Relationship between respiratory microbiota and tumor infiltrating lymphocytes in patients with non-small-cell lung cancer. A, Boxplot of CD8⁺ T cell density in treatment responders (R) and nonresponders (NR). $0.001 \leq P < .01$ by Mann-Whitney test. B, Pairwise Spearman's rank correlation heatmap between featured respiratory microbes and CD4⁺ T cells, CD8⁺ T cells, IFN- γ ⁺CD4⁺ T cells (Th1), IL-4⁺CD4⁺ T cells (Th2), FoxP3⁺CD4⁺ T cells (Treg). $0.001 \leq P < .01$. C, Univariate linear regression between CD8⁺ T cell density and the abundance of Streptococcus. D, Representative CD8⁺ immunohistochemistry images showing high and low abundance of Streptococcus groups

bronchial lavage fluid by bronchoscope can avoid the problem, it only reflects the LRT microbiota and is challenging to carry out, with poor patient compliance. Sampling on the posterior pharyngeal wall with a pharyngeal swab can only reflect the URT microbiota, and there was also the great possibility that the samples were contaminated by oral microbiota. Given all these concerns,

we took sputum samples as the research medium based on the following considerations: sputum could reflect the whole respiratory microbiota landscape to the greatest extent as sputum expectorates from the LRT to URT. Oral microbiota has been found not related to the anti-PD-1 response.¹⁶ We additionally compared profiles between the oral microbiota and sputum microbiota in 24

patients. Results showed that there was a difference between the two. A clustering heatmap analysis of the top 20 most abundant microbes showed that some microbes between the two groups seemed unbalanced (Figure S5A). The featured microbes in the two groups were presented by LEfSe analysis (Figure S5B). Although there was no difference in alpha diversity between the two, beta diversity analysis by PCoA based on weighted UniFrac distance showed a significant difference ($P < .01$), which indicated that the two communities had different species evolution patterns (Figure S5C,D).

In this study, we found that the abundance of nearly all favorable microbes featured in R and unfavorable microbes featured in NR at the genus level were significantly correlated with PS scores. Better PS seemed to potentially boost favorable microbes or decrease unfavorable microbes to improve anti-PD-1 response. According to our results, patients with better PS seem to be more likely to be recommended for anti-PD-1 treatment from the gut microbiota perspective. These findings are consistent with NCCN guidelines recommending patients with better PS (PS scores 0-1) to receive anti-PD-1 treatment.

In conclusion, as a biomarker with the ability to maintain relatively stable characteristics during anti-PD-1 treatment, the gut and paired respiratory microbiota are important in identifying suitable candidates who could benefit from anti-PD-1 treatment. Additionally, considering the characteristic of plasticity, the commensal microbiota might be an alternative option to regulate the clinical effects of ICIs.

ACKNOWLEDGMENTS

This study was supported by the Medicine and Health Science Technology Development Project of Shandong Province (2019WS204), the Natural Science Foundation of Shandong Province (ZR2020QH209), and the National Natural Science Foundation of China (Grant nos. 81774198 and 81573871). We also appreciate the great technical support from the Public Platform of Medical Research Center, Academy of Chinese Medical Science, Zhejiang Chinese Medical University.

DISCLOSURE

The authors have no conflict of interest.

ORCID

Chufeng Zhang  <https://orcid.org/0000-0002-9268-7748>

REFERENCES

- Reck M, Rodríguez-Abreu D, Robinson AG, et al. Pembrolizumab versus chemotherapy for PD-L1-positive non-small-cell lung cancer. *N Engl J Med*. 2016;375(19):1823-1833.
- Postow MA, Chesney J, Pavlick AC, et al. Nivolumab and ipilimumab versus ipilimumab in untreated melanoma. *N Engl J Med*. 2015;372(21):2006-2017.
- Ansell SM, Lesokhin AM, Borrello I, et al. PD-1 blockade with nivolumab in relapsed or refractory Hodgkin's lymphoma. *N Engl J Med*. 2015;372(4):311-319.
- Borghaei H, Paz-Ares L, Horn L, et al. Nivolumab versus docetaxel in advanced nonsquamous non-small-cell lung cancer. *N Engl J Med*. 2015;373(17):1627-1639.
- Powles T, Staehler M, Ljungberg B, et al. Updated EAU guidelines for clear cell renal cancer patients who fail VEGF targeted therapy. *Eur Urol*. 2016;69(1):4-6.
- Pardoll D. Cancer and the immune system: basic concepts and targets for intervention. *Semin Oncol*. 2015;42(4):523-538.
- Schadendorf D, Hodi FS, Robert C, et al. Pooled analysis of long-term survival data from phase II and phase III trials of ipilimumab in unresectable or metastatic melanoma. *J Clin Oncol*. 2015;33(17):1889-1894.
- Robert C, Ribas A, Schachter J, et al. Pembrolizumab versus ipilimumab in advanced melanoma (KEYNOTE-006): post-hoc 5-year results from an open-label, multicentre, randomised, controlled, phase 3 study. *Lancet Oncol*. 2019;20(9):1239-1251.
- Mok T, Wu YL, Kudaba I, et al. Pembrolizumab versus chemotherapy for previously untreated, PD-L1-expressing, locally advanced or metastatic non-small-cell lung cancer (KEYNOTE-042): a randomised, open-label, controlled, phase 3 trial. *Lancet*. 2019;393(10183):1819-1830.
- Rizvi NA, Hellmann MD, Snyder A, et al. Cancer immunology. Mutational landscape determines sensitivity to PD-1 blockade in non-small cell lung cancer. *Science*. 2015;348(6230):124-128.
- Riaz N, Havel JJ, Kendall SM, et al. Recurrent SERPINB3 and SERPINB4 mutations in patients who respond to anti-CTLA4 immunotherapy. *Nat Genet*. 2016;48(11):1327-1329.
- Schumacher TN, Schreiber RD. Neoantigens in cancer immunotherapy. *Science*. 2015;348(6230):69-74.
- Carbone DP, Reck M, Paz-Ares L, et al. First-line nivolumab in stage IV or recurrent non-small-cell lung cancer. *N Engl J Med*. 2017;376(25):2415-2426.
- Smyth MJ, Ngiu SF, Ribas A, Teng MW. Combination cancer immunotherapies tailored to the tumour microenvironment. *Nat Rev Clin Oncol*. 2016;13(3):143-158.
- Koyama S, Akbay EA, Li YY, et al. Adaptive resistance to therapeutic PD-1 blockade is associated with upregulation of alternative immune checkpoints. *Nat Commun*. 2016;7:10501.
- Gopalakrishnan V, Spencer CN, Nezi L, et al. Gut microbiome modulates response to anti-PD-1 immunotherapy in melanoma patients. *Science*. 2018;359(6371):97-103.
- Routy B, Le Chatelier E, Derosa L, et al. Gut microbiome influences efficacy of PD-1-based immunotherapy against epithelial tumors. *Science*. 2018;359(6371):91-97.
- Matson V, Fessler J, Bao R, et al. The commensal microbiome is associated with anti-PD-1 efficacy in metastatic melanoma patients. *Science*. 2018;359(6371):104-108.
- Sivan A, Corrales L, Hubert N, et al. Commensal Bifidobacterium promotes antitumor immunity and facilitates anti-PD-L1 efficacy. *Science*. 2015;350(6264):1084-1089.
- Jin Y, Dong H, Xia L, et al. The diversity of gut microbiome is associated with favorable responses to anti-programmed death 1 immunotherapy in Chinese patients with NSCLC. *J Thorac Oncol*. 2019;14(8):1378-1389.
- Jin C, Lagoudas GK, Zhao C, et al. Commensal microbiota promote lung cancer development via $\gamma\delta$ T cells. *Cell*. 2019;176(5):998-1013.e16.
- Eisenhauer EA, Therasse P, Bogaerts J, et al. New response evaluation criteria in solid tumours: revised RECIST guideline (version 1.1). *Eur J Cancer*. 2009;45(2):228-247.
- Schwartz LH, Litière S, de Vries E, et al. RECIST 1.1-Update and clarification: from the RECIST committee. *Eur J Cancer*. 2016;62:132-137.
- Sharma P, Retz M, Siefker-Radtke A, et al. Nivolumab in metastatic urothelial carcinoma after platinum therapy (CheckMate

- 275): a multicentre, single-arm, phase 2 trial. *Lancet Oncol.* 2017;18(3):312-322.
25. Chen P-L, Roh W, Reuben A, et al. Analysis of immune signatures in longitudinal tumor samples yields insight into biomarkers of response and mechanisms of resistance to immune checkpoint blockade. *Cancer Discov.* 2016;6(8):827-837.
26. Arbour KC, Mezquita L, Long N, et al. Impact of baseline steroids on efficacy of programmed cell death-1 and programmed death-ligand 1 blockade in patients with non-small-cell lung cancer. *J Clin Oncol.* 2018;36(28):2872-2878.
27. Derosa L, Hellmann MD, Spaziano M, et al. Negative association of antibiotics on clinical activity of immune checkpoint inhibitors in patients with advanced renal cell and non-small-cell lung cancer. *Ann Oncol.* 2018;29(6):1437-1444.
28. Shaverdian N, Lisberg AE, Bornazyan K, et al. Previous radiotherapy and the clinical activity and toxicity of pembrolizumab in the treatment of non-small-cell lung cancer: a secondary analysis of the KEYNOTE-001 phase 1 trial. *Lancet Oncol.* 2017;18(7):895-903.
29. Hastings K, Yu HA, Wei W, et al. EGFR mutation subtypes and response to immune checkpoint blockade treatment in non-small-cell lung cancer. *Ann Oncol.* 2019;30(8):1311-1320.
30. Chao A. Non-parametric estimation of the number of classes in a population. *Scand J Stat.* 1984;11:265-270.
31. Kim B-R, Shin J, Guevarra RB, et al. Deciphering diversity indices for a better understanding of microbial communities. *J Microbiol Biotechnol.* 2017;27(12):2089-2093.
32. Tanoue T, Morita S, Plichta DR, et al. A defined commensal consortium elicits CD8 T cells and anti-cancer immunity. *Nature.* 2019;565(7741):600-605.
33. Iida N, Dzutsev A, Stewart CA, et al. Commensal bacteria control cancer response to therapy by modulating the tumor microenvironment. *Science.* 2013;342(6161):967-970.
34. Reese AT, Dunn RR. Drivers of microbiome biodiversity: a review of general rules, feces, and ignorance. *MBio.* 2018;9(4):e01294-18.
35. Yatsunenko T, Rey FE, Manary MJ, et al. Human gut microbiome viewed across age and geography. *Nature.* 2012;486(7402):222-227.
36. Man WH, de Steenhuijsen Pijters WA, Bogaert D. The microbiota of the respiratory tract: gatekeeper to respiratory health. *Nat Rev Microbiol.* 2017;15(5):259-270.
37. Kostic AD, Gevers D, Pedamallu CS, et al. Genomic analysis identifies association of *Fusobacterium* with colorectal carcinoma. *Genome Res.* 2012;22(2):292-298.
38. Bullman S, Pedamallu CS, Sicinska E, et al. Analysis of *Fusobacterium* persistence and antibiotic response in colorectal cancer. *Science.* 2017;358(6369):1443-1448.
39. Kostic A, Chun E, Robertson L, et al. *Fusobacterium nucleatum* potentiates intestinal tumorigenesis and modulates the tumor-immune microenvironment. *Cell Host Microbe.* 2013;14(2):207-215.
40. Yu TaChung, Guo F, Yu Y, et al. *Fusobacterium nucleatum* promotes chemoresistance to colorectal cancer by modulating autophagy. *Cell.* 2017;170(3):548-563.e16.

SUPPORTING INFORMATION

Additional supporting information may be found online in the Supporting Information section.

How to cite this article: Zhang C, Wang J, Sun Z, Cao Y, Mu Z, Ji X. Commensal microbiota contributes to predicting the response to immune checkpoint inhibitors in non-small-cell lung cancer patients. *Cancer Sci.* 2021;112:3005-3017. <https://doi.org/10.1111/cas.14979>